J Geod (2013) 87:539–553
DOI 10.1007/s00190-013-0630-7

ORIGINAL ARTICLE

Ambiguity resolution for triple-frequency geometry-free and ionosphere-free combination tested with real data

K. Wang · M. Rothacher

Received: 24 August 2012 / Accepted: 18 February 2013 / Published online: 9 April 2013

Abstract The recent GPS Block IIF satellites SVN62 and SVN63 and the Galileo satellites GIOVE-A, GIOVE-B, PFM and FM2 already send signals on more than two frequencies, and more GNSS satellites will provide tracking data on at least three frequencies in the near future. In this paper, a simplified general method for ambiguity resolution minimizing the noise level for the triple-frequency geometry-free (GF) and ionosphere-free (IF) linear combinations is presented, where differently scaled code noise on the three frequencies was introduced. For the third of three required linear combinations, the most demanding one in triple-frequency ambiguity resolution, we developed a general method using the ambiguity-corrected phase observations without any constraints to search for the optimal GF and IF linear combination. We analytically demonstrate that the noise level of this third linear combination only depends on the three frequencies. The investigation concerning this frequency-dependent noise factor was performed for GPS, Galileo and Compass frequency triplets. We verified the theoretical derivations with real triple-frequency GPS and Galileo data from the Multi-GNSS Experiment (M–GEX) of the International GNSS Service (IGS). The data of about 30 M–GEX stations around the world over 11 days from 29 April 2012 to 9 May 2012 were used for the test. For the third linear combinaton using Galileo E1, E5b and E5a, which is expected to have the worst performance among all the GNSS frequency triplets in our investigation, the formal errors of the estimated ambiguities are in most cases below 0.2 cycles after 400 observation epochs. If more GPS satellites sending signals on three frequencies or more stations tracking Galileo E6 signal are available in the future, an improvement by a factor of two to three can be expected.

Keywords Triple-frequency ambiguity resolution · Geometry-free and ionosphere-free · Linear combination · GNSS

K. Wang (✉) · M. Rothacher
Institute of Geodesy and Photogrammetry, ETH Zurich,
Schafmattstr.34, 8093 Zurich, Switzerland
e-mail: wangk@ethz.ch

M. Rothacher
e-mail: markus.rothacher@ethz.ch

1 Introduction

Nowadays, different GNSS already provide or will provide their tracking data on three or even four frequencies. It is, thus, interesting to exploit the advantages of the increasing number of frequencies and search for geometry-free (GF) and ionosphere-free (IF) linear combinations with minimized noise. Hatch (2006) introduced a method for obtaining triple-frequency GF, refraction-corrected, ambiguity-resolved carrier-phase measurements. Feng et al. (2007) provided a model using the differences between geometry-based (GB), i.e. the geometry-related terms were preserved, triple-frequency code observations and GB triple-frequency phase observations to form geometry-free linear combinations, and their differences were investigated with respect to their ionospheric refractions and noise levels. Recently, Henkel and Günther (2012) introduced a more general method that uses simultaneously multi-frequency code and phase observations allowing an arbitrary scaling of the geometry, the ionospheric delay and the minimized noise level. The code noise on the three frequencies was assumed to be scaled according to the Cramer Rao bounds (CRB) (Henkel and Günther 2012). In this paper here, we present a simplified method for GF and IF linear combinations using simultaneously triple-frequency code and phase observations with different sets of scaling factors for the code noise. For given

integer coefficients of the three ambiguities, the optimized combination with the minimized combined noise can be expressed as a function of the three frequencies and the scaling factors of the code noise on the three frequencies. Different sets of scaling factors were tested with real triple-frequency Galileo data.

The GF and IF linear combination is useful especially for the case of long baselines (e.g. a global network), where the first-order term of the ionospheric delays cannot be fully eliminated, and for the case of Wide Area Real Time Kinematics (WARTK) measurements, where the geometry-related information such as the orbits, the clocks and the troposphere parameters are not available precisely enough and sometimes need to be estimated. In the case of Precise Point Positioning (PPP), the method can only be used when the satellite- and receiver-related biases are stable enough and can be estimated before the ambiguity resolution.

In order to solve the ambiguities, three linearly independent combinations are necessary. Various studies have been done in recent years to find the third GF and IF linear combination with acceptable noise. The ambiguity-corrected phase observations were used instead of the code observations to significantly reduce the noise level of the combination, and three sets of GB phase linear combinations were proposed to form a geometry-free linear combination (Li et al. 2010). Apart from that, Li et al. 2012 established a GF and IF approach for narrow-lane ambiguity resolution. In this study here, a more general method using ambiguity-corrected phase observations is used to form the third linear combination. It is analytically demonstrated that the noise level after combination is only a function of the three frequencies. This frequency-dependent factor is investigated for different GNSS. The Galileo combination using E1, E6 and E5a has the smallest frequency-dependent factor and the best behavior among all the systems.

The theoretical derivations were verified with real data. The data were processed for 11 days in 2012 and the fractional parts and formal errors of the estimated ambiguities for all the three linear combinations were investigated.

2 GF and IF triple-frequency linear combinations

Ignoring hardware delays, multipath errors and higher-order terms of the ionospheric refraction, the code and phase observation equations of a specific carrier frequency on the zero-difference level can be described as follows:

$$P_i = \rho + I_1 \cdot \frac{f_1^2}{f_i^2} + \delta_{tro} + c \cdot \delta_r - c \cdot \delta^s + \epsilon_P,$$

$$L_i = \rho - I_1 \cdot \frac{f_1^2}{f_i^2} + \delta_{tro} + c \cdot \delta_r - c \cdot \delta^s + \lambda_i \cdot n_i + \epsilon_L, \qquad (1)$$

where P_i and L_i represent the code and phase observation on frequency f_i, respectively. The symbol ρ is the distance from the satellite at the epoch of transmission to the receiver at the epoch of reception. δ_{tro}, δ_r and δ^s stand for the tropospheric delay, receiver clock correction and satellite clock correction, respectively. I_1 is the first-order term of the ionospheric refraction on carrier L_1 and c is the speed of light. ϵ_P and ϵ_L stand for the code and phase observation errors, respectively. λ_i represents the wavelength of the signal on frequency f_i and n_i represents the ambiguity on frequency f_i.

If the phase and code observations are available on three frequencies, it is possible to generate linear combinations that are both, GF and IF, i.e. they eliminate all geometry-related terms and the first-order ionospheric refraction. With the help of Eq. 1, the most general linear combination that can be formed using the code and phase observations on three carrier frequencies is given by:

$$\begin{aligned} L_x &= \gamma_1 L_1 + \gamma_2 L_2 + \gamma_3 L_3 + \gamma_4 P_1 + \gamma_5 P_2 + \gamma_6 P_3 \\ &= (\gamma_1 + \gamma_2 + \gamma_3 + \gamma_4 + \gamma_5 + \gamma_6)(\rho + \delta_{tro} + c\delta_r - c\delta^s) \\ &\quad + (\gamma_4 + \frac{f_1^2}{f_2^2}\gamma_5 + \frac{f_1^2}{f_3^2}\gamma_6 - \gamma_1 - \frac{f_1^2}{f_2^2}\gamma_2 - \frac{f_1^2}{f_3^2}\gamma_3) I_1 \\ &\quad + (\gamma_1\lambda_1 n_1 + \gamma_2\lambda_2 n_2 + \gamma_3\lambda_3 n_3) + \epsilon, \end{aligned} \qquad (2)$$

where L_x is the combined observation. γ_i $(i = 1, \ldots, 6)$ represent the weighting coefficients of the three phase and the three code observations. ϵ stands for the observation error after combination.

The combined ambiguity n_x, which is a linear combination of the ambiguities n_1, n_2 and n_3, has to be an integer for ambiguity resolution purposes:

$$\begin{aligned} \lambda_x n_x &= \gamma_1\lambda_1 n_1 + \gamma_2\lambda_2 n_2 + \gamma_3\lambda_3 n_3 \\ &= \lambda_x(a_x \cdot n_1 + b_x \cdot n_2 + c_x \cdot n_3), \end{aligned} \qquad (3)$$

where λ_x represents the wavelength after combination. a_x, b_x and c_x are integer coefficients of the phase combinations on three frequencies.

As a result of Eq. 3, we obtain the following relationships between the weighting coefficients γ_1, γ_2 and γ_3 and the integer coefficients a_x, b_x and c_x (Henkel and Günther 2010):

$$\gamma_1 = \frac{a_x f_1}{f_x}, \quad \gamma_2 = \frac{b_x f_2}{f_x}, \quad \gamma_3 = \frac{c_x f_3}{f_x}. \qquad (4)$$

Compared to the method, where a GB code combination is subtracted from a GB phase combination (Feng et al. 2007), the general combination described above has the advantage of being more general and not losing any degrees of freedom. Apart from that, the weighting coefficients γ_4, γ_5 and γ_6 of the code observations do not have to follow the same relationship as those of the phase observations (see Eq. 4).

In order to generate a GF linear combination, the factor appearing before the geometry-related terms (see Eq. 2) has

to be zero. Using Eq. 4, the following equation for the weighting coefficients γ_4, γ_5 and γ_6 of the code observations can be derived:

$$\frac{a_x f_1 + b_x f_2 + c_x f_3}{f_x} + \gamma_4 + \gamma_5 + \gamma_6 = 0. \tag{5}$$

An IF linear combination requires the factor before I_1 (see Eq. 2) to be zero. With the help of Eq. 4, the following equation can be derived:

$$\gamma_4 + \frac{f_1^2}{f_2^2}\gamma_5 + \frac{f_1^2}{f_3^2}\gamma_6 = \frac{f_1}{f_x}(a_x + b_x\frac{f_1}{f_2} + c_x\frac{f_1}{f_3}). \tag{6}$$

With Eqs. 5 and 6, the code weighting coefficients γ_4 and γ_5 can be expressed as functions of γ_6:

$$\gamma_4 = \frac{m_1}{f_x} + m_2\gamma_6, \quad \gamma_5 = \frac{m_3}{f_x} + m_4\gamma_6, \tag{7}$$

with

$$m_1 = \frac{f_1((f_1^2+f_2^2)f_3a_x + 2f_1f_2f_3b_x + (f_2^2+f_3^2)f_1c_x)}{f_3(f_2^2-f_1^2)},$$

$$m_2 = -\frac{f_1^2(f_2^2-f_3^2)}{f_3^2(f_2^2-f_1^2)},$$

$$m_3 = \frac{f_2((f_1^2+f_2^2)f_3b_x + 2f_1f_2f_3a_x + (f_1^2+f_3^2)f_2c_x)}{f_3(f_1^2-f_2^2)},$$

$$m_4 = -\frac{f_2^2(f_1^2-f_3^2)}{f_3^2(f_1^2-f_2^2)},$$

where m_1 and m_3 are functions of the three frequencies and the integer coefficients a_x, b_x and c_x with the characteristics $m_1(-a_x,-b_x,-c_x) = -m_1(a_x,b_x,c_x)$ and $m_3(-a_x,-b_x,-c_x) = -m_3(a_x,b_x,c_x)$. m_2 and m_4 are just functions of the three carrier frequencies f_1, f_2 and f_3.

2.1 Minimizing the noise level of the GF and IF triple-frequency linear combinations

Henkel and Günther 2012 has introduced a general method to minimize the noise level of the multi-frequency code carrier linear combinations. In this section, an algorithm limited to triple-frequency GF and IF linear combinations is discussed. The results of this algorithm for different frequency triplets using different scaling factors for the code noise are shown in Sec. 2.2.

Since the code observation noise is dominant in the combined noise, the minimal code observation noise after combination is of great interest. Assuming that the code noise on the three carrier frequencies σ_{P1}, σ_{P2} and σ_{P3} can be formulated with three scaling factors C_4, C_5 and C_6 and an unscaled code observation noise σ_P in meters:

$$\sigma_{P1} = C_4\sigma_P, \quad \sigma_{P2} = C_5\sigma_P, \quad \sigma_{P3} = C_6\sigma_P, \tag{8}$$

the so-called code noise amplification factor N_{Code} can be formulated as follows:

$$\begin{aligned} N_{Code} &= \sqrt{C_4^2\gamma_4^2 + C_5^2\gamma_5^2 + C_6^2\gamma_6^2} \\ &= \sqrt{C_4^2(\frac{m_1}{f_x} + m_2\gamma_6)^2 + C_5^2(\frac{m_3}{f_x} + m_4\gamma_6)^2 + C_6^2\gamma_6^2} \\ &= \sqrt{(m_2^2C_4^2 + m_4^2C_5^2 + C_6^2)(\gamma_6 + \frac{m_1m_2C_4^2 + m_3m_4C_5^2}{f_x(m_2^2C_4^2 + m_4^2C_5^2 + C_6^2)})^2 + \frac{1}{f_x^2}N_{MIN}}, \end{aligned} \tag{9}$$

with

$$\begin{aligned} N_{MIN} &= m_1^2C_4^2 + m_3^2C_5^2 - \frac{(m_1m_2C_4^2 + m_3m_4C_5^2)^2}{m_2^2C_4^2 + m_4^2C_5^2 + C_6^2} \\ &= \frac{(m_1m_4 - m_2m_3)^2C_4^2C_5^2 + m_1^2C_4^2C_6^2 + m_3^2C_5^2C_6^2}{m_2^2C_4^2 + m_4^2C_5^2 + C_6^2} \geq 0, \end{aligned}$$

and the combined code noise σ_{Code}^C expressed in cycles of λ_x can be formulated as:

$$\begin{aligned} \sigma_{Code}^C &= N_{Code}\frac{\sigma_P}{\lambda_x} = N_{Code}\frac{\sigma_P f_x}{c} \\ &= \frac{\sigma_P}{c}\sqrt{(m_2^2C_4^2 + m_4^2C_5^2 + C_6^2)f_x^2(\gamma_6 + \frac{m_1m_2C_4^2 + m_3m_4C_5^2}{f_x(m_2^2C_4^2 + m_4^2C_5^2 + C_6^2)})^2 + N_{MIN}}. \end{aligned} \tag{10}$$

Equation 10 shows that both, the code noise amplification factor N_{Code} and the combined code noise σ_{Code}^C, are the square root of a quadratic polynomial in γ_6, and are minimal, if

$$\gamma_6 = -\frac{m_1m_2C_4^2 + m_3m_4C_5^2}{(m_2^2C_4^2 + m_4^2C_5^2 + C_6^2)f_x}. \tag{11}$$

In this case, we have

$$\sigma_{Code}^C = \frac{\sigma_P}{c}\sqrt{N_{MIN}}, \tag{12}$$

where the value N_{MIN} is independent of the combined frequency f_x. Expressed in another way, the minimal σ_{Code}^C can be determined, when the integer coefficients a_x, b_x and c_x for the phase observations and the scaling factors C_4, C_5 and C_6 are given. At the same time, all six weighting coefficients γ_i ($i = 1,\ldots,6$) are given up to a common factor f_x (see Eqs. 4, 7 and 11), that does not affect N_{MIN}.

The phase noise plays only a secondary role compared to the code noise, but it still needs to be considered. Assuming that the phase observation noise is identical in either meters or cycles for all the three frequencies, it turns out that the combined phase noise σ_{Phase}^C in cycles is also independent of the combined frequency f_x:

$$\sigma_{Phase}^{C} = \frac{\sqrt{\gamma_1^2+\gamma_2^2+\gamma_3^2}\cdot\sigma_L}{\lambda_x} = \frac{\sqrt{a_x^2 f_1^2+b_x^2 f_2^2+c_x^2 f_3^2}\cdot\sigma_L}{c}, \quad or$$
$$\sigma_{Phase}^{C} = \frac{\sqrt{\gamma_1^2\lambda_1^2+\gamma_2^2\lambda_2^2+\gamma_3^2\lambda_3^2}\cdot\sigma_L^C}{\lambda_x} = \sigma_L^C\sqrt{a_x^2+b_x^2+c_x^2}, \tag{13}$$

where σ_L and σ_L^C represent the phase observation noise of the three carrier frequencies in meters and in cycles, respectively.

The entire combined noise σ^C in cycles is, thus, also independent of the combined frequency f_x and can be formulated as:

$$\sigma^C = \sqrt{(\sigma_{Code}^C)^2 + (\sigma_{Phase}^C)^2}. \tag{14}$$

To eliminate receiver and satellite electronic delays, typically double differences are formed for ambiguity resolution. Assuming that the linearly combined measurements have a white noise, the formal errors σ_{Amb}^{CD} (in cycles) of the ambiguity estimates on the double-difference level decrease inversely proportional to the square root of the number of observation epochs n:

$$\sigma_{Amb}^{CD} = \frac{2\sqrt{(\sigma^C)^2 + (\sigma_{MP}^C)^2}}{\sqrt{n}}, \tag{15}$$

where σ_{MP}^C represents the multipath errors in cycles for each station. In Eq. 15, it is assumed that both stations have uncorrelated code and phase noise and multipath errors. The factor of two in Eq. 15 results from forming of double-differences.

With the assumption that the observation noise has a normal (Gaussian) distribution, the probability for correct ambiguity-fixing, namely the success rate, can be calculated according to Wang et al. (2004):

$$P_{correct}^{D} = P(|x| < \frac{1}{2}) = P(|z| < \frac{1}{2\sigma_{Amb}^{CD}}), \tag{16}$$

where $P_{correct}^{D}$ represents the probabilities for a correct ambiguity-fixing on the double-difference level, and x and z stand for the unnormalized and normalized fractional parts of the ambiguity estimates in cycles, respectively.

The probability of correctly fixing the ambiguity is then calculated with the cumulative distribution function of the standardized normal distribution $\Phi(m)$:

$$P(|z| < m) = \Phi(m) - (1 - \Phi(m)) = 2\Phi(m) - 1, \tag{17}$$

with

$$\Phi(m) = \frac{1}{2}\left(1 + \mathrm{erf}\left(\frac{m}{\sqrt{2}}\right)\right),$$

where erf is the error function, and m stands for $\frac{1}{2(\sigma_{Amb}^{CD})}$ in our case.

2.2 The best GF and IF triple-frequency linear combinations for different GNSS frequency triplets

To find the IF and GF triple-frequency combinations for GPS signals at L1($f_1 = 1575.42$ MHz), L2($f_2 = 1227.6$ MHz) and L5($f_3 = 1176.45$ MHz) with the lowest σ^C in cycles, the integer coefficients a_x, b_x and c_x were varied in the range of -10 to $+10$. A phase observation noise of $\sigma_L = 0.01$ cycles was assumed. For the code observation noise, two different sets of scaling factors C_4, C_5 and C_6 were tested. The first set assumes an identical noise level of $\sigma_P = 0.5\,m$ for all three frequencies ($C_4 = C_5 = C_6 = 1$). The best four combinations resulting in this case are listed in the top part of Table 1. The second set uses scaling factors according to the CRB (Henkel and Günther 2012) with $\sigma_P = 2\,m$, $C_4 = C_5 = 0.2592$ and $C_6 = 0.0783$ leading to the four combinations given in the bottom part of Table 1. The entire combined noise values σ^C and σ_{CRB}^C in cycles for these two cases are shown in the sixth column of Table 1. The six weighting coefficients $\gamma_i (i = 1, \ldots, 6)$ are listed in the third, fourth and fifth column. The wavelength of the linear combinations was set to 1 m. The success rates on the double-difference level with 1 and 10 observation epochs for these two cases are documented in the last two columns. The combinations with opposite signs for a_x, b_x and c_x, which deliver the same σ^C and σ_{CRB}^C, are not listed in Table 1.

The triple-frequency combinations using code and phase observations simultaneously are not only eliminating the first-order term of the ionospheric refraction and all the geometry-related terms, but they are also reducing the code noise significantly. Compared to the Melbourne-Wübbena combination for double frequencies, which leads to a noise of $\sigma^C = 0.4136$ cycles with the assumption that the code and phase noise equals 0.5 m and 0.01 cycles, respectively, we can benefit more from the triple-frequency linear combinations such as (0,−1,1) with $\sigma^C = 0.0615$ cycles and (1,−4,3) with $\sigma^C = 0.3517$ cycles. We can also see that σ_{CRB}^C for the linear combination (0,−1,1) is much smaller than σ^C, because the observation noise assumed for L5 is much smaller. However, for the other linear combinations, σ_{CRB}^C does not seem to benefit a lot from this smaller noise on L5.

Apart from GPS, the Galileo system will provide signals at E1(1575.42 MHz), E6(1278.75 MHz), E5b(1207.14 MHz), E5(1191.795 Hz) and E5a(1176.45 MHz), and the Chinese Compass system will also transmit multi-frequency signals. The combinations for Galileo, named GalileoA (E1, E6 and E5b), GalileoB (E1, E6 and E5), GalileoC (E1, E6 and E5a) and GalileoD (E1, E5b and E5a), as well as the triple-frequency combination for Compass-III (B1 at 1575.42 MHz, B3 at 1268.52 MHz and B2 at 1191.795 MHz)

Table 1 IF and GF triple-frequency combinations for GPS with small combined noise

$a_x,\ b_x,\ c_x$	$\gamma_i (i = 1, \cdots, 6)$				$\sigma^C \& \sigma^C_{CRB}$	$P^D_{correct}$ (%)	
					(cycles)	$n = 1$	$n = 10$
$C_4 = C_5 = C_6 = 1$							
0, −1, 1	$\gamma_{1,2,3}$	0.0000	−4.0948	3.9242	0.0615	100.0	100.0
	$\gamma_{4,5,6}$	0.0021	0.0759	0.0926			
1, −4, 3	$\gamma_{1,2,3}$	5.2550	−16.3793	11.7726	0.3517	52.28	97.54
	$\gamma_{4,5,6}$	−0.6880	−0.0521	0.0917			
1, −3, 2	$\gamma_{1,2,3}$	5.2550	−12.2845	7.8484	0.3529	52.13	97.49
	$\gamma_{4,5,6}$	−0.6901	−0.1280	−0.0009			
1, −5, 4	$\gamma_{1,2,3}$	5.2550	−20.4742	15.6969	0.3612	51.12	97.14
	$\gamma_{4,5,6}$	−0.6859	0.0238	0.1844			
$C_4 = C_5 = 0.2592 \quad C_6 = 0.0783$							
0, −1, 1	$\gamma_{1,2,3}$	0.0000	−4.0948	3.9242	0.0284	100.0	100.0
	$\gamma_{4,5,6}$	0.0136	0.0132	0.1438			
1, −6, 5	$\gamma_{1,2,3}$	5.2550	−24.5690	19.6211	0.3551	51.86	97.40
	$\gamma_{4,5,6}$	−0.6493	−0.0878	0.4299			
1, −7, 6	$\gamma_{1,2,3}$	5.2550	−28.6638	23.5453	0.3560	51.75	97.36
	$\gamma_{4,5,6}$	−0.6356	−0.0746	0.5737			
1, −5, 4	$\gamma_{1,2,3}$	5.2550	−20.4742	15.6969	0.3564	51.69	97.34
	$\gamma_{4,5,6}$	−0.6629	−0.1010	0.2862			

(Li et al. 2012) were investigated with respect to their noise values. The phase observation noise is set to be 0.01 cycles, while the code observation noise is set to be $\sigma_P = 0.5$ m with scaling factors $C_4 = C_5 = C_6 = 1$ for the first case and $\sigma_P = 2$ m with scaling factors proportional to the CRB for the second case. The CRB for the Galileo signals are 11.14 cm for E1, 1.95 cm for E5, 7.83 cm for E5a and E5b and 11.36 cm for E6 (Henkel and Günther 2012). For each system, the two linear combinations with the lowest combined noise are listed in Table 2.

We see that for all investigated GNSS, the combined ambiguities can be rounded to the nearest integers with high success rates after only about 10 observation epochs. Looking at the second best linear combination, Compass-III and most of the Galileo combinations show a better performance than GPS. The σ^C_{CRB} is generally much smaller than σ^C, because the code observation noise assumed in the case of CRB is much smaller than $\sigma_P = 0.5$ m. As long as we do not know the real noise level of the triple-frequency observations, it is hard to decide which of the two selections of scaling factors is more suitable for minimizing the combined noise level of the linear combinations. Therefore, both selections were tested with real data (see Sec. 4).

3 Resolving ambiguities on the three carrier frequencies

In order to resolve all three ambiguities n_1, n_2 and n_3, three linearly independent linear combinations are required. It is hard, however, to find a third linear combination, because all the combinations with relatively low noise are linearly dependent on the first two combinations given in Tables 1 and 2. For this reason, significant research has been performed in recent years to form a third linear combination with relatively low noise. In this section, the results of such an investigation are shown using a general linear combination of the phase observations on three carrier frequencies.

The resolved combined ambiguities from the first two linear combinations, n_x and n_y, are introduced as known into the third linear combination with the ambiguity named n_z:

$$\begin{aligned} n_x &= a_x n_1 + b_x n_2 + c_x n_3, \quad n_y = a_y n_1 + b_y n_2 + c_y n_3, \\ n_z &= a_z n_1 + b_z n_2 + c_z n_3 \\ &= \frac{b_z c_y - c_z b_y}{b_x c_y - c_x b_y} n_x + \frac{b_z c_x - c_z b_x}{b_y c_x - c_y b_x} n_y + Q(a_z, b_z, c_z) n_1, \end{aligned} \tag{18}$$

with

$$Q(a_z, b_z, c_z) = a_z - a_x \frac{b_z c_y - c_z b_y}{b_x c_y - c_x b_y} - a_y \frac{b_z c_x - c_z b_x}{c_x b_y - b_x c_y}.$$

This means that the integer coefficients a_z, b_z and c_z of the third linear combination do not necessarily have to be integers; only a linear combination of a_z, b_z and c_z, here called $Q(a_z, b_z, c_z)$, has to be integer. Because the third linear combination is linearly independent of the first two, the integer $Q(a_z, b_z, c_z)$ is not allowed to be zero.

If the integer coefficients of the first two linear combinations have the pattern $(u, v, -(u + v))$ as listed in Tables 1

Table 2 IF and GF triple-frequency linear combinations for different GNSS with small combined noise

a_x, b_x, c_x	σ^C	$P^D_{correct}$ [%]		a_x, b_x, c_x	σ^C_{CRB}	$P^D_{\mathrm{correct,CRB}}$[%]	
	[cycle]	$n=1$	$n=10$	(CRB)	[cycle]	$n=1$	$n=10$
GalileoA (E1, E6 and E5b)							
0, −1, 1	0.0844	99.70	100.0	0, −1, 1	0.0323	100.0	100.0
1, −3, 2	0.3023	59.17	99.11	1, −3, 2	0.1370	93.19	100.0
GalileoB (E1, E6 and E5)							
0, −1, 1	0.1014	98.63	100.0	0, −1, 1	0.0195	100.0	100.0
1, −2, 1	0.3061	58.58	99.02	1, −5, 4	0.1279	94.94	100.0
GalileoC (E1, E6 and E5a)							
0, −1, 1	0.1182	96.56	100.0	0, −1, 1	0.0431	100.0	100.0
1, −2, 1	0.3068	58.49	99.00	1, −2, 1	0.1379	93.02	99.64
GalileoD (E1, E5b and E5a)							
0, −1, 1	0.0388	100.0	100.0	0, −1, 1	0.0181	100.0	100.0
1, −5, 4	0.3697	50.12	96.75	1, −3, 2	0.1686	86.18	100.0
Compass-III (B1, B3 and B2)							
0, −1, 1	0.0901	99.45	100.0				
1, −3, 2	0.3148	57.29	98.80				

and 2 (see also the pattern found by Cocard et al. (2008) for the promising triple-frequency GF carrier phase linear combinations), the function $Q(a_z, b_z, c_z)$ always equals $a_z + b_z + c_z$, which means $a_z + b_z + c_z$ has to be an integer. Let us call this integer I:

$$I = a_z + b_z + c_z. \tag{19}$$

In order to further reduce the noise, the so-called ambiguity-corrected phase observations from the first two linear combinations can be used instead of the code observations (Li et al. 2010). The phase observations on the three carriers f_1, f_2 and f_3, and both of the ambiguity-corrected combined phase observations $\tilde{L}_x$ and $\tilde{L}_y$ are again combined linearly:

$$L_z = \gamma_{z1}L_1 + \gamma_{z2}L_2 + \gamma_{z3}L_3 + q_1\tilde{L}_x + q_2\tilde{L}_y, \tag{20}$$

with

$$\tilde{L}_x = \gamma_{x1}L_1 + \gamma_{x2}L_2 + \gamma_{x3}L_3 - n_x\lambda_x, \quad \text{and}$$
$$\tilde{L}_y = \gamma_{y1}L_1 + \gamma_{y2}L_2 + \gamma_{y3}L_3 - n_y\lambda_y,$$

where γ_{xi}, γ_{yi} and γ_{zi} (i=1,2,3) represent the phase weighting coefficients for the three linear combinations, respectively. q_1 and q_2 stand for the weighting coefficients of the ambiguity-corrected phase observations from the first two linear combinations. It should be noted that the ambiguity-corrected phase observations $\tilde{L}_x$ and $\tilde{L}_y$ are neither GF nor IF.

In order to generate an IF and GF combination according to Eq. 20, the following two criteria must be fulfilled (see Eqs. 4, 5 and 6):

$$\frac{g_z}{f_z} + q_1\frac{g_x}{f_x} + q_2\frac{g_y}{f_y} = 0, \tag{21}$$

with

$$g_i = a_i f_1 + b_i f_2 + c_i f_3, \quad i = x, y, z,$$

and

$$\frac{h_z}{f_z} + q_1\frac{h_x}{f_x} + q_2\frac{h_y}{f_y} = 0, \tag{22}$$

with

$$h_i = a_i + b_i\frac{f_1}{f_2} + c_i\frac{f_1}{f_3}, \quad i = x, y, z.$$

The parameters q_1 and q_2 can be calculated as

$$q_1 = \frac{f_x(g_y h_z - g_z h_y)}{f_z(g_x h_y - g_y h_x)}, \quad q_2 = -\frac{f_y(g_x h_z - g_z h_x)}{f_z(g_x h_y - g_y h_x)}. \tag{23}$$

In order to calculate the entire combined noise, Eq. 20 can then be expressed based only on the phase observations on the three frequencies:

$$L_z = (\gamma_{z1}+q_1\gamma_{x1}+q_2\gamma_{y1})L_1 + (\gamma_{z2}+q_1\gamma_{x2}+q_2\gamma_{y2})L_2 + (\gamma_{z3}+q_1\gamma_{x3}+q_2\gamma_{y3})L_3 - q_1 n_x\lambda_x - q_2 n_y\lambda_y. \tag{24}$$

Assuming that the phase observation noise on the three carriers is identical and amounts to σ_L in meters or σ^C_L in cycles, the entire combined noise σ^C_z in cycles of λ_1 (see Eqs. 18, 19 and 24) for the third linear combination can then be calculated as:

$$\sigma_z^C = \frac{f_z \cdot \sigma_L \sqrt{s_a f_1^2 + s_b f_2^2 + s_c f_3^2}}{|I| \cdot c}, \quad \text{or}$$
$$\sigma_z^C = \frac{f_z \cdot \sigma_L^C \sqrt{s_a + s_b + s_c}}{|I|}, \tag{25}$$

with

$$s_a = \left(\frac{a_z}{f_z} + q_1 \frac{a_x}{f_x} + q_2 \frac{a_y}{f_y}\right)^2,$$
$$s_b = \left(\frac{b_z}{f_z} + q_1 \frac{b_x}{f_x} + q_2 \frac{b_y}{f_y}\right)^2,$$
$$s_c = \left(\frac{c_z}{f_z} + q_1 \frac{c_x}{f_x} + q_2 \frac{c_y}{f_y}\right)^2.$$

Inserting Eq. 23 into 25, we obtain the equations

$$s_a = \frac{p_a}{f_z^2}, \quad s_b = \frac{p_b}{f_z^2}, \quad s_c = \frac{p_c}{f_z^2}, \tag{26}$$

with

$$p_a = \left(a_z + a_x \frac{g_y h_z - g_z h_y}{g_x h_y - g_y h_x} - a_y \frac{g_x h_z - g_z h_x}{g_x h_y - g_y h_x}\right)^2,$$
$$p_b = \left(b_z + b_x \frac{g_y h_z - g_z h_y}{g_x h_y - g_y h_x} - b_y \frac{g_x h_z - g_z h_x}{g_x h_y - g_y h_x}\right)^2,$$
$$p_c = \left(c_z + c_x \frac{g_y h_z - g_z h_y}{g_x h_y - g_y h_x} - c_y \frac{g_x h_z - g_z h_x}{g_x h_y - g_y h_x}\right)^2,$$

where p_a, p_b and p_c are functions of the three carrier frequencies f_1, f_2 and f_3 and the integer coefficients a_i, b_i and c_i $(i = x, y, z)$. They are independent of the three combined frequencies f_x, f_y and f_z.

Inserting Eq. 26 into 25, we obtain:

$$\sigma_z^C = \frac{\sigma_L \sqrt{p_a f_1^2 + p_b f_2^2 + p_c f_3^2}}{|I| \cdot c}, \quad \text{or}$$
$$\sigma_z^C = \frac{\sigma_L^C \sqrt{p_a + p_b + p_c}}{|I|}. \tag{27}$$

We see that σ_z^C (in cycles of λ_1) is independent of the combined frequencies f_x, f_y and f_z. From Eqs. 18, 19 and 23, it is not hard to get:

$$g_i(-a_i, -b_i, -c_i) = -g_i(a_i, b_i, c_i),$$
$$h_i(-a_i, -b_i, -c_i) = -h_i(a_i, b_i, c_i),$$
$$p_a(-a_i, -b_i, -c_i) = p_a(a_i, b_i, c_i),$$
$$p_b(-a_i, -b_i, -c_i) = p_b(a_i, b_i, c_i),$$
$$p_c(-a_i, -b_i, -c_i) = p_c(a_i, b_i, c_i), \quad i = x, y, z. \tag{28}$$

As a result, σ_z^C will not be affected if all the signs of the integer coefficients a_i, b_i and c_i are changed simultaneously:

$$\sigma_z^C(-a_i, -b_i, -c_i) = \sigma_z^C(a_i, b_i, c_i). \tag{29}$$

Equation 27 can also be formulated with the phase observation noise and a noise factor μ or μ^C:

$$\sigma_z^C = \sigma_L \cdot \mu = \sigma_L^C \cdot \mu^C, \tag{30}$$

with

$$\mu := \frac{\sqrt{p_a f_1^2 + p_b f_2^2 + p_c f_3^2}}{|I| \cdot c}, \quad \mu^C := \frac{\sqrt{p_a + p_b + p_c}}{|I|}.$$

If the integer coefficients (a_x, b_x, c_x) and (a_y, b_y, c_y) of the first two linear combinations follow the pattern $(u, v, -(u+v))$ as in Tables 1 and 2, the noise factors μ and μ^C are independent of the integer coefficients a_i, b_i and c_i $(i = x, y, z)$. This conclusion agrees with the results of Li et al. (2010). We get

$$\mu = \frac{\sqrt{f_1^4(f_2^2-f_3^2)^2 + f_2^4(f_1^2-f_3^2)^2 + f_3^4(f_1^2-f_2^2)^2}}{|(f_1-f_2)(f_1-f_3)(f_2-f_3)| \cdot c},$$
$$\mu^C = \frac{\sqrt{f_1^2(f_2^2-f_3^2)^2 + f_2^2(f_1^2-f_3^2)^2 + f_3^2(f_1^2-f_2^2)^2}}{|(f_1-f_2)(f_1-f_3)(f_2-f_3)|}. \tag{31}$$

σ_z^C (in cycles of λ_1) was calculated for different GNSS frequency triplets with a pre-defined phase observation noise $\sigma_L = 5$ mm or $\sigma_L^C = 0.01$ cycles. The results are shown in Table 3. The second and the fourth column list σ_z^C with $\sigma_L = 5$ mm and $\sigma_L^C = 0.01$ cycles, while the third and fifth column document the corresponding noise factors μ and μ^C. We see that the third linear combinations of Compass-III, GalileoA, GalileoB and GalileoC reach a lower noise factor than GPS. The noise factors μ and μ^C for GalileoC with E1, E6 and E5a are about 40% smaller than those for GPS.

The formal errors of the n_1 ambiguity estimates decrease with an increasing number of observation epochs (see Eq. 15). Figure 1 (top) shows the formal errors σ_{Amb}^{CD} of the n_1 ambiguity estimates on the double-difference level for different GNSS frequency triplets ignoring the multipath errors because of the low weighting coefficients of the code observations (see Table 1). The noise level of the phase observations is set to be $\sigma_L^C = 0.01$ cycles. We immediately see that the combinations GalileoA, GalileoB, GalileoC and Compass-III show an even better behavior than GPS. For GalileoC (black line) σ_{Amb}^{CD} is lower than 0.2 cycles after 213 epochs and reaches about 0.13 cycles after 500 epochs. The formal errors of the n_1 ambiguity estimates are also directly related to the success rates (see Eq. 16) of the ambiguity resolution, which are shown in Fig. 1 (bottom) with $\sigma_L = 0.01$ cycles. We conclude that under the assumptions made, the success rates for GalileoB (green line), GalileoC (black line) and Compass-III (yellow line) are above 90% after 200 epochs.

Table 3 Combined noise and the noise factors of the third linear combination for different GNSS frequency triplets

	$\sigma_L = 5$ mm σ_z^C (cycles)	μ	$\sigma_L = 0.01$ cycles σ_z^C (cycles)	μ^C
GPS (L1,L2,L5)	5.0676	1,013.5	2.5082	250.8
GalileoA (E1,E6,E5b)	4.5348	907.0	2.1542	215.4
GalileoB (E1,E6,E5)	3.6707	734.1	1.7431	174.3
GalileoC (E1,E6,E5a)	3.0754	615.1	1.4588	145.9
GalileoD (E1,E5b,E5a)	7.9361	1,587.2	3.9813	398.1
Compass-III (B1,B3,B2)	3.9918	798.4	1.9123	191.2

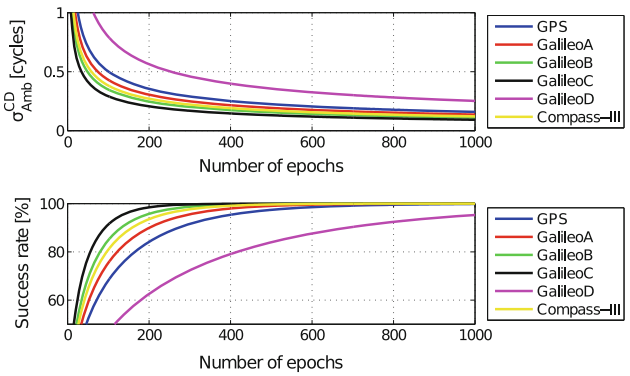

Fig. 1 Formal errors of the n_1 ambiguity estimates (*top*) and the success rates (*bottom*) as a function of the number n of observation epochs

4 The best linear combination after resolving all three ambiguities

After resolving n_1 according to Sec. 3, the other two ambiguities n_2 and n_3 can easily be computed using the resolved combined ambiguities n_x and n_y (see Eq. 18). Making use of our knowledge of all three integers n_1, n_2 and n_3, we are now looking for the best IF and GB linear combination with minimized noise in meters.

With the help of Eq. 1, the triple-frequency phase linear combination can be formulated as:

$$\begin{aligned} L_P &= \gamma_1 L_1 + \gamma_2 L_2 + \gamma_3 L_3 - (\gamma_1\lambda_1 n_1 + \gamma_2\lambda_2 n_2 + \gamma_3\lambda_3 n_3) \\ &= (\gamma_1 + \gamma_2 + \gamma_3)(\rho + \delta_{tro} + c\delta_r - c\delta^s) \\ &\quad -(\gamma_1 + \frac{f_1^2}{f_2^2}\gamma_2 + \frac{f_1^2}{f_3^2}\gamma_3)I_1, \end{aligned} \tag{32}$$

where L_P represents the triple-frequency phase linear combination.

Li et al. (2012) have shown that the coefficients γ_1, γ_2 and γ_3 are just functions of the three frequencies. The minimal combined noise values σ^{MD}_{min} in meters for different GNSS frequency triplets on the double-difference level are listed in Table 4 with the assumption that the phase observation noise is 0.01 cycles on each of the three frequencies. After resolving the three ambiguities, the minimized noise of the phase GB and IF linear combination is then about 1 cm for all the investigated GNSS frequency triplets.

5 Verification with real data

The theoretical derivations of the GF and IF triple-frequency linear combinations were verified with real GPS and Galileo data. The two GPS–IIF satellites PRN01 (SVN63) and PRN25 (SVN62) are sending signals on the three frequencies f_1, f_2 and f_5 (USNO 2012). Both of the GIOVE (Galileo In-Orbit Validation Element) satellites, GIOVE–A and GIOVE–B, and the two Galileo In-Orbit Validation (IOV) satellites (PFM and FM2), which were launched in October 2011, are also providing signals on more than two frequencies (Inside GNSS 2012). The 24-h Multi-GNSS Experiment (M–GEX) data (Weber 2012) with a sampling rate of 30 s were collected for the period 29 April 2012 to 9 May 2012 from the IGS website ftp://cddis.gsfc.nasa.gov/pub/gps/data/campaign/mgex/daily/rinex3/2012 (Noll et al. 2009) in the format RINEX 3.00 (Gurtner 2007; Januszewski 2011). About 30 M–GEX stations were available in this time period (see Fig. 2).

Table 4 Minimized combined noise of the GB and IF linear combination after solving the three ambiguities in meters on the double-difference level for different GNSS

	γ_1	γ_2	γ_3	σ^{MD}_{min} (m)
GPS (L1,L2,L5)	2.3522	−0.4964	−0.8557	0.0102
GalileoA (E1,E6,E5b)	2.5422	−0.4559	−1.0863	0.0113
GalileoB (E1,E6,E5)	2.4510	−0.3679	−1.0831	0.0109
GalileoC (E1,E6,E5a)	2.3604	−0.2875	−1.0729	0.0106
GalileoD (E1,E5b,E5a)	2.3241	−0.5591	−0.7649	0.0101
Compass-III (B1,B3,B2)	2.4521	−0.4159	−1.0362	0.0109

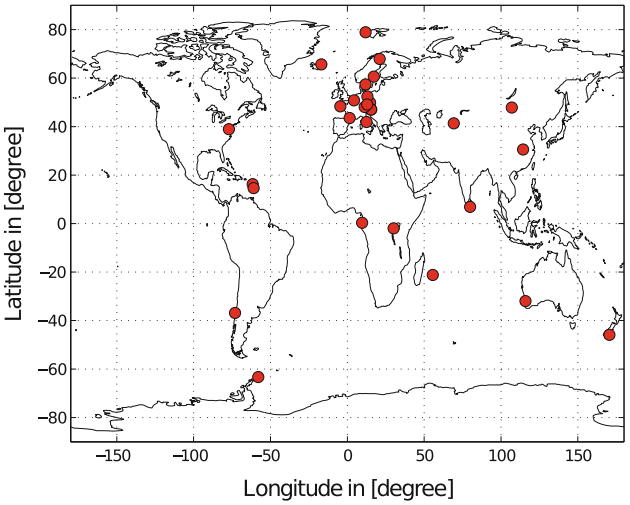

Fig. 2 Multi-GNSS experiment (M–GEX) stations on 29 April 2012

5.1 Fractional parts and formal errors of n_x and n_y

In order to form double-differenced triple-frequency linear combinations, at least two satellites of each system providing more than two frequencies have to be available. The two GPS–IIF satellites PRN01 and PRN25 can only be observed simultaneously from two stations during a short time interval at low elevation angles, while a relatively long overlapping time can be found for E11 (Galileo–IOV satellite PFM), E12 (Galileo–IOV satellite FM2) and E52 (GIOVE–B satellite) in the available M–GEX dataset. Because no signal on frequency E6 was recorded simultaneously for two stations with a baseline shorter than 1,000 km, the frequency combination GalileoD (E1, E5b, E5a) (see Fig. 1; Tables 2, 3) was used for the processing of Galileo baselines. An elevation mask of 6° was set for all satellites. The observations were weighted with the elevation angle β_E according to

$$P_{Z_r^s} = \sin(\beta_E)^2,$$
$$P_D = \frac{1}{\frac{1}{P_{Z_1^1}} + \frac{1}{P_{Z_1^2}} + \frac{1}{P_{Z_2^1}} + \frac{1}{P_{Z_2^2}}}, \tag{33}$$

where $P_{Z_r^s}$ and P_D represent the weight of the observations on the zero-difference and double-difference level.

Figure 3 shows the fractional parts and the formal errors of the estimated n_x and n_y for two Galileo baselines, namely ons1 (Onsala, Sweden) – mar7 (Gavle, Sweden) with a baseline length of 470 km and brux (Brussels, Belgium) – grab (Graz, Austria) with a baseline length of 913 km (see Fig. 3a , b) as well as for two GPS baselines ons1–mar7 and kir8 (Kiruna, Sweden) – mar7 with a baseline length of 832 km (see Fig. 3c, d). Generally speaking, the estimated n_x and n_y from the first two GF and IF linear combinations mostly have an absolute fractional part below 0.2 cycles with a formal error smaller than 0.1 cycles. We see that the formal errors decrease with increasing number of observation epochs and are mostly below or around the expected values (red line and blue line; according to Eq. 15) except for some outliers generated by the Galileo baseline brux–grab. It is not hard to see that for the Galileo linear combinations, the results generated from baseline brux–grab are generally worse than the results of the baseline ons1–mar7. The reason certainly is that different tracking modes or channels for the same frequency (Gurtner 2007) exhibit biases that do not cancel by double-differencing. In addition, since different antenna types are part of the baseline brux–grab, Phase Center Variations (PCVs) may also lead to deviations from integers. It should be noted that signals were received on the same channels for the Galileo baseline ons1–mar7 (E1X, E5bX, E5aX), but at different channels for the baseline brux–grab with E1C, E5bQ and E5aQ for station brux and E1X, E5bX, E5aX for station grab. For the GPS baselines, the results using the channels (L1C, L2W, L5X) are plotted.

5.2 Impact of receiver tracking modes on n_x and n_y

To have a closer look at the differences in the results caused using different tracking channels, the fractional parts and the formal errors of the estimated n_x and n_y ambiguities were compared using different tracking channels for both of the GPS baselines. Only identical ambiguities (same baseline, same day and same number of observation epochs) were compared and the standard deviations of the absolute fractional parts (see column 2 and 3) and the standard deviations of the formal errors (column 4 and 5) for each tracking channel combination are listed in Table 5. We see that the fractional n_x of the combination L1C, L2W and L5X for one station and L1C, L2X and L5X for the other station are the smallest for the case of 45 epochs, while using channels L1C, L2W and L5X for both stations seems to be the best choice for 160 epochs. Among different choices of tracking channels, we did not observe big differences for the formal errors. As expected, the formal errors of the linear combinations with about 160 epochs are generally smaller than those with only 45 epochs. The scaling factors of the formal errors between the two cases are bigger than the expected scaling factors $\sqrt{160/45}$ because of the elevation dependency. For the case of 160 epochs, the elevation angles are generally larger than for the 45 epoch case. We also see that the real errors (column 2 and 3) are slightly smaller than the formal errors (column 4 and 5) for the case of 45 epochs and bigger than the formal errors for the case of 160 epochs. The systematic effects (such as multipath errors) play a more and more important role as the time interval considered is increasing. A more concrete investigation concerning the channel combinations will be possible, if more M–GEX data is available in the future.

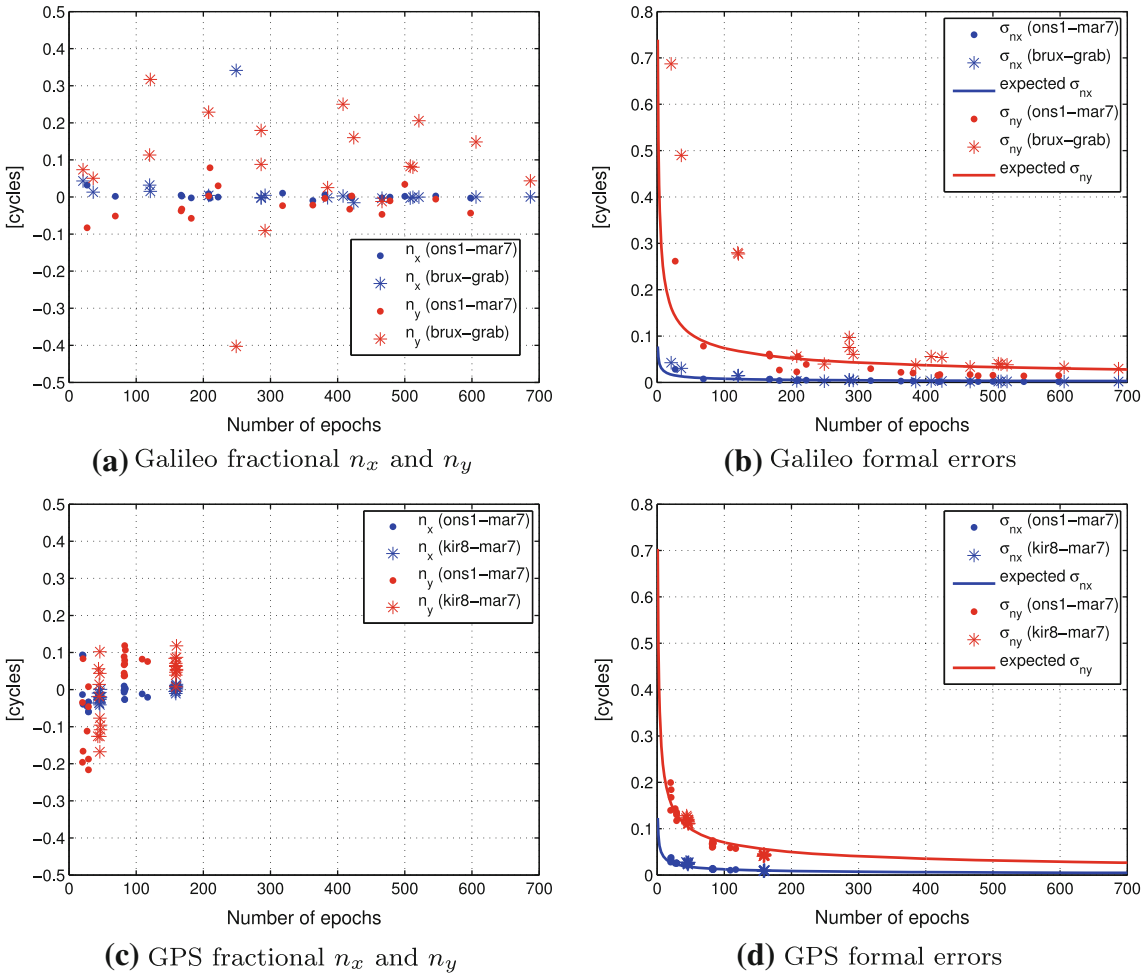

(a) Galileo fractional n_x and n_y

(b) Galileo formal errors

(c) GPS fractional n_x and n_y

(d) GPS formal errors

Fig. 3 Fractional parts (**a**), (**c**) and formal errors (**b**), (**d**) of the estimated n_x and n_y for the Galileo baselines ons1–mar7 and brux–grab and for the GPS baselines ons1–mar7 and kir8–mar7 from 30 April 2012 to 9 May 2012

Table 5 Standard deviations of the absolute values of the fractional parts n_x and n_y and standard deviations of their formal errors for different channel combinations with different numbers of observation epoches

	Δn_x (cycles)	Δn_y (cycles)	σ_{nx} (cycles)	σ_{ny} (cycles)
Number of observation epochs: ca. 45				
L1C,L2W,L5X – L1C, L2W, L5X	0.0254	0.0932	0.0255	0.1169
L1C,L2X,L5X – L1C, L2X, L5X	0.0190	0.0902	0.0232	0.1180
L1C,L2W,L5X – L1C, L2X, L5X	0.0178	0.0974	0.0247	0.1181
L1C,L2X,L5X – L1C, L2W, L5X	0.0433	0.0866	0.0243	0.1168
Number of observation epochs: ca. 160				
L1C,L2W,L5X – L1C, L2W, L5X	0.0082	0.0782	0.0095	0.0425
L1C,L2X,L5X – L1C, L2X, L5X	0.0126	0.0606	0.0087	0.0431
L1C,L2W,L5X – L1C, L2X, L5X	0.0357	0.0541	0.0093	0.0431
L1C,L2X,L5X – L1C, L2W, L5X	0.0198	0.0847	0.0090	0.0425

5.3 Scaling factors for the code noise

As discussed in Sec. 2, two different sets of scaling factors for the code observation noise on the three frequencies, namely the identical scaling factors $C_4 = C_5 = C_6 = 1$ and the scaling factors according to CRB, were tested with real data. Since the overlapping time interval for the observation of the two GPS satellites PRN01 and PRN25 is very short for

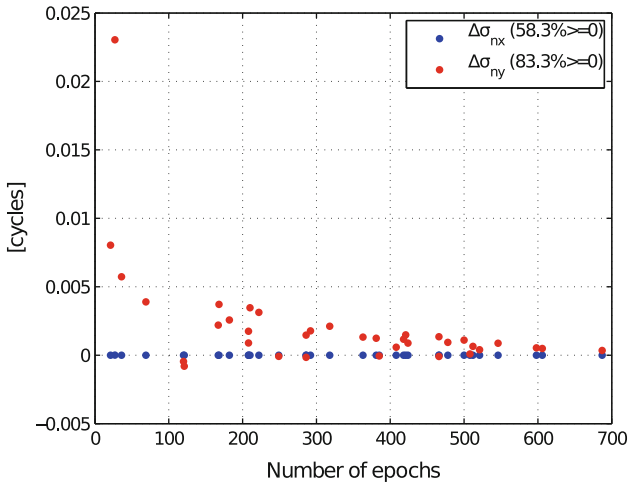

Fig. 4 Differences of the formal errors for the first two linear combinations using the CRB and identical scaling factors for Galileo baselines ons1–mar7 and brux–grab from 29 April 2012 to 9 May 2012

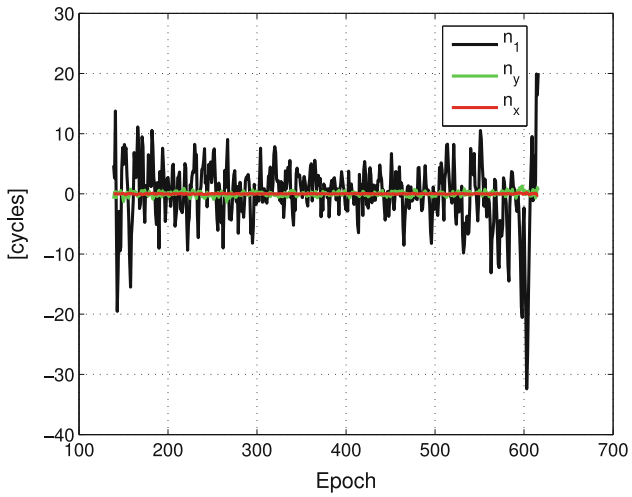

Fig. 5 The three linear combinations used for fixing n_x, n_y and n_1 for baseline ons1–mar7 and satellites E11 and E52 between 1:09 and 5:08 am on 29 April 2012

most of the baselines, only real data of the Galileo satellites from 29 April 2012 to 9 May 2012 was used for this analysis. The differences in the formal errors using the two sets of scaling factors (CRB scaling factors minus identical scaling factors) are shown in Fig. 4. We see that in most of the cases, using identical scaling factors generates smaller formal errors for the combined ambiguity n_y of the second linear combination, especially for ambiguities n_y with short observation intervals. For the first linear combination, the case using identical scaling factors is also slightly better than using the CRB scaling factors. This gives a hint that the actual measurement noise levels of the code observations on different frequencies should be studied more carefully. In view of the better performance, the ambiguities n_x and n_y based on $C_4 = C_5 = C_6 = 1$ were thus introduced for the analysis of the third linear combination.

5.4 The third linear combination

The linear combinations of the real observation data which were used to fix n_x, n_y and n_1 for the baseline ons1–mar7 and satellites E11 and E52 between 1:09 and 5:08 am on 29 April 2012 are shown in Fig. 5 as an example. The third linear combination L_z^{CD} was corrected by $\frac{b_z c_y - c_z b_y}{b_x c_y - c_x b_y} n_x + \frac{b_z c_x - c_z b_x}{b_y c_x - c_y b_x} n_y$ and divided by the integer I (see Eq. 18). We see that the core problem of triple-frequency ambiguity resolution is fixing the ambiguities n_1 with the third linear combination.

The triple-frequency combinations for the baselines ons1–mar7 and brux–grab on 29 April 2012 are listed in Table 6. The frequencies on L1, L2 and L5 and on E1, E5b and E5a were available and used when forming triple-frequency linear combinations. In Table 6, the channels which generate the lowest formal error for n_1 on 29 April 2012 were selected for each baseline. The second and fourth column document the fractional parts of the estimated combined ambiguities n_x and n_y, and the third and fifth column list their corresponding formal errors. The estimated n_1 from the third linear combination and its formal error are listed in the sixth and seventh column, and the last column lists the expected formal errors σ_{n1}^E of n_1 calculated with the theoretical derivations (see Eqs. 15, 30) based on the assumption that the phase observation noise is 0.01 cycles and independent of the elevation angle.

We see that for the third combined ambiguity, the formal error is sometimes bigger than expected and sometimes smaller. The relatively big formal error of n_1 is very likely caused by the real observation noise, which is bigger than expected, or the effects that are included in the observation noise such as, e.g. multipath errors. To have a closer look, Fig. 6a, b shows the third combined observation L_z^{CD} in cycles on the double-difference level divided by the factor μ^C for different pairs of stations and satellites. An offset was subtracted for each pair and each time interval. The elevation angles for the two Galileo baselines are shown in Fig. 6c, d. We see an obvious correlation between the elevation angles, the observation noise and the formal errors of the estimated n_1.

The standard deviation σ_L^{CD} of the combined phase observations $\frac{L_z^{CD}}{\mu^C}$ in Fig. 6a, b and the mean values of the elevation-dependent weights of the double-differenced observations are given in Table 7. The expected phase observation noise σ_L^{ECD} on the double-difference level is 0.02 cycles.

It is not hard to see that the real noise for short observation intervals is in some cases bigger than 0.02 cycles due to the low elevation angles (small weights), which results in relatively big formal errors in Table 6.

Table 6 The estimated ambiguities and their formal errors for three linearly independent combinations on the double-difference level using M–GEX data on 29 April 2012

Number of epochs	n_x (cycles)	σ_{nx} (cycles)	n_y (cycles)	σ_{ny} (cycles)	n_1 (cycles)	σ_{n1} (cycles)	σ_{n1}^E (cycles)
ons1–mar7 (470 km) G01, G25 (L1C, L2X, L5X – L1C, L2W, L5X)							
127	−0.0234	0.0110	0.0891	0.0588	−0.2511	0.5938	0.4451
kir8–mar7 (832 km) G01, G25 (L1C, L2X, L5X – L1C, L2W, L5X)							
159	−0.0186	0.0093	0.0790	0.0412	−0.3252	0.5109	0.3978
47	−0.0387	0.0251	−0.0745	0.1106	0.3466	1.3730	0.7317
ons1–mar7 (470 km) E11, E52 (E1X, E5bX, E5aX – E1X, E5bX, E5aX)							
478	−0.0005	0.0018	−0.0103	0.0144	0.1667	0.1864	0.3642
168	0.0026	0.0072	−0.0326	0.0568	−0.1184	0.7364	0.6143
brux–grab (913 km) E11, E12 (E1C, E5bQ, E5aQ – E1X, E5bX, E5aX)							
466	−0.0032	0.0018	−0.0123	0.0334	−0.3812	0.1594	0.3689
121	0.0153	0.0147	0.3171	0.2771	0.0640	1.3219	0.7239

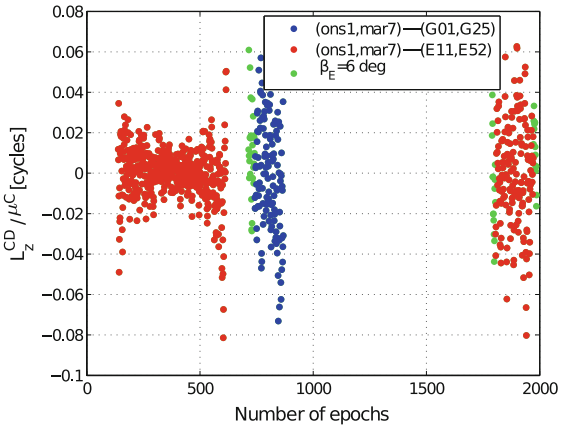

(a) $\frac{L_z^{CD}}{\mu^C}$ for ons1–mar7

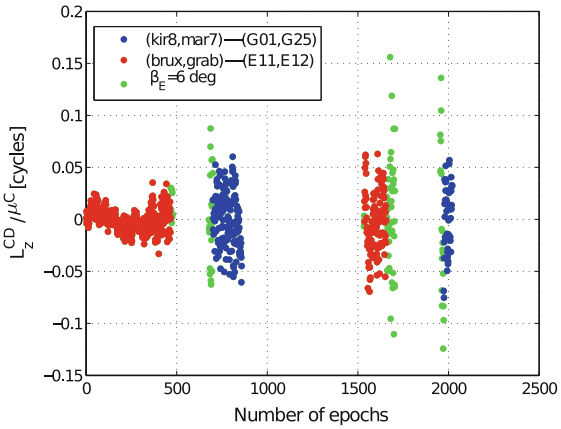

(b) $\frac{L_z^{CD}}{\mu^C}$ for kir8–mar7 and brux–grab

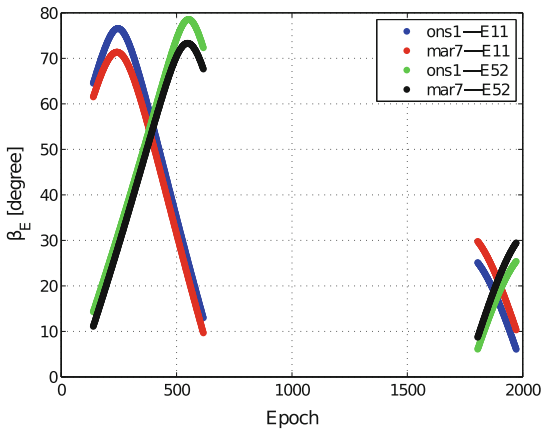

(c) Elevation of ons1–mar7

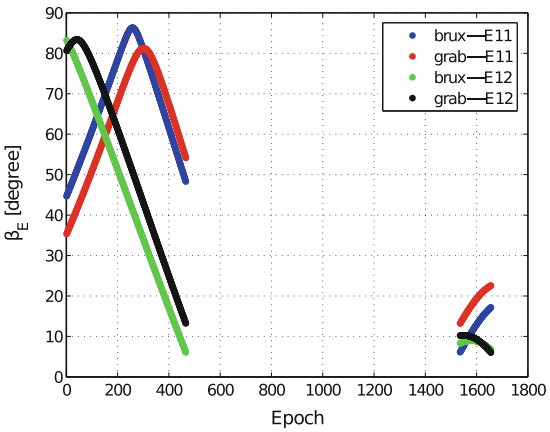

(d) Elevation of kir8–mar7 and brux–grab

Fig. 6 The third combined observation L_z^{CD} in cycles on the double-difference level divided by factor μ^C for baseline **a** ons1–mar7 and **b** kir8–mar7 and brux–grab and the corresponding elevation angles for the two Galileo baselines **c** ons1–mar7 and **d** brux–grab on 29 April 2012. The *green dots* represent the observations with an elevation angle lower than 6°

Table 7 Real phase observation noise for some double-differenced observations on 29 April 2012

Baseline	Satellites	Number of epochs	σ_L^{CD} (cycles)	P_D (Eq. 33)	σ_L^{ECD} (cycles)
ons1–mar7 (470 km)	G01, G25	127	0.0269	0.0128	0.0200
	E11, E52	478	0.0133	0.1042	0.0200
		168	0.0259	0.0190	0.0200
kir8–mar7 (832 km)	G01, G25	159	0.0265	0.0197	0.0200
		47	0.0323	0.0092	0.0200
brux–grab (913 km)	E11, E12	466	0.0102	0.1393	0.0200
		121	0.0291	0.0078	0.0200

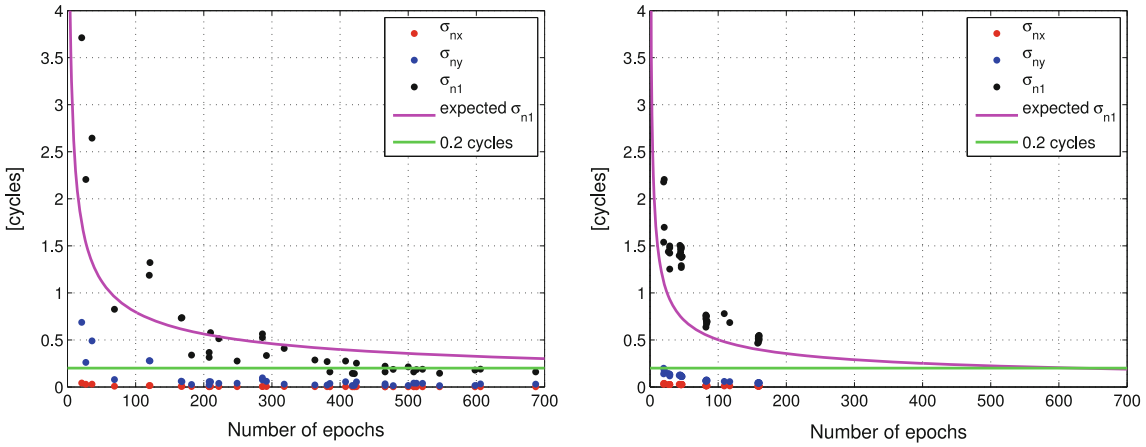

(a) Galileo baselines **(b)** GPS baselines

Fig. 7 Formal errors of estimated n_x, n_y and n_1 for Galileo baselines ons1–mar7 and brux–grab and GPS baselines ons1–mar7 and kir8–mar7 from 29 April 2012 to 9 May 2012

Figure 7 shows the formal errors of the estimated n_x, n_y and n_1 for (a) the two Galileo baselines and (b) the two GPS baselines for the time period from 29 April 2012 to 9 May 2012. The red, blue and black dots represent the formal errors of the estimated n_x, n_y and n_1, respectively. The magenta lines stand for the expected formal errors of n_1 with the assumption that the phase observation noise equals 0.01 cycles on the zero-difference level. They correspond to the magenta line (Galileo) and the blue line (GPS) in Fig. 1 (top). The green line marks the boundary of 0.2 cycles for the formal errors. We see that the formal errors decrease with an increasing number of observation epochs. n_x and n_y, which are determined from the first two linear combinations, are generally much easier to be fixed than n_1 from the third linear combination. Most of the formal errors for n_1 are below or around the expected values, which suggests a phase observation noise around or lower than the assumed 0.01 cycles, except for some cases with short observation intervals and low elevation angles. The formal errors for n_1 are mostly below 0.2 cycles, if the number of observation epochs is larger than 400 epochs.

Table 8 lists the real errors, i.e. the absolute fractional parts, and the formal errors of the estimated n_x, n_y and n_1 for the cases with more than 400 observation epochs for both of the Galileo baselines. We see that the real errors are mostly smaller than 0.01 cycles for n_x and 0.15 cycles for n_y. The real errors for the first two linear combinations are sometimes bigger than the formal errors, but do not affect the fixing of n_x and n_y. For the third linear combination, the real errors are about 67% bigger than the formal errors and are sometimes bigger than 0.3 cycles. The systematic effects, such as multipath errors, that are present in the phase-only observations, result in difficulties for the ambiguity resolution of n_1. We also see that the behavior of the baseline ons1–mar7 is much better than the baseline brux–grab for both, the second and the third linear combination. The biases caused by different tracking channels (see Sec. 5.2) and, possibly, PCVs caused by different antenna types play an important role in ambiguity resolution.

However, with more and more Galileo and GPS satellites providing three frequencies in the near future, longer observation times including also higher elevation angles can be

Table 8 Real and formal errors of the estimated n_x, n_y and n_1 for both of the Galileo baselines with more than 400 observation epochs

Number of epochs	$\lvert\delta n_x\rvert$ (cycles)	σ_{nx} (cycles)	$\lvert\delta n_y\rvert$ (cycles)	σ_{ny} (cycles)	$\lvert\delta n_1\rvert$ (cycles)	σ_{n1} (cycles)
ons1–mar7						
418	0.0008	0.0020	0.0327	0.0153	0.1152	0.1443
421	0.0028	0.0018	0.0026	0.0168	0.2949	0.1418
466	0.0020	0.0020	0.0469	0.0168	0.3854	0.2210
478	0.0005	0.0018	0.0103	0.0144	0.1667	0.1864
500	0.0017	0.0020	0.0342	0.0154	0.1872	0.2132
546	0.0026	0.0015	0.0058	0.0140	0.2781	0.1451
598	0.0026	0.0016	0.0436	0.0150	0.1367	0.1792
brux–grab						
408	0.0028	0.0031	0.2499	0.0558	0.3949	0.2758
424	0.0156	0.0031	0.1600	0.0537	0.3015	0.2522
466	0.0032	0.0018	0.0123	0.0334	0.3812	0.1594
508	0.0031	0.0018	0.0825	0.0404	0.3839	0.1595
512	0.0009	0.0023	0.0802	0.0393	0.1572	0.1847
521	0.0003	0.0021	0.2056	0.0381	0.4465	0.1882
606	0.0000	0.0019	0.1483	0.0326	0.3810	0.1897
687	0.0003	0.0018	0.0436	0.0295	0.2971	0.1594

expected. It will, thus, be possible to obtain a higher success rate for fixing n_1 in the third linear combination, i.e. more n_1 ambiguities with a formal error lower than 0.2 cycles will result. To achieve better results, it will also be necessary to calibrate the PCVs as well as the differential code biases (DCBs) between channels. Furthermore, if the signals on E6 from the Galileo satellites and the signals on B1, B3 and B2 from the Compass-III satellites can be received by more stations in the future, the linear combinations of GalileoA, GalileoB, GalileoC and Compass-III (see Table 3) will be able to generate much better results for n_1, namely better by a factor of two to three.

6 Summary and conclusions

In this work, we presented a simplified method for ambiguity resolution using triple-frequency GF and IF linear combinations. The code and phase observations on the three frequencies were simultaneously used to identify the two GF and IF linear combinations with the lowest noise level. It has been demonstrated that the noise level after forming the linear combinations is independent of the combined wavelength. The third linear combination with a low noise level is much more difficult to be found and poses the core problem in triple-frequency ambiguity resolution. A general method using the ambiguity-corrected phase observations without any constraints was used to search for the optimal GF and IF linear combination. We analytically demonstrated that the combined noise level is only a function of the three frequencies and not depending on the details of the linear combination. The resulting frequency-dependent factor was investigated for different GNSS frequency triplets. The Galileo combination using E1, E6 and E5a shows the best behavior among all the systems.

The theoretical derivations were verified with real data. Different scaling factors for the code noise on the three frequencies were set and tested. Using identical scaling factors has been shown to be better than using scaling factors derived from the CRB of the signals, especially for the second linear combination. The formal errors of the estimated ambiguities using E1, E5b and E5a, which is expected to show the worst performance among different GNSS triple-frequency combinations in our investigation, are mostly better than expected and below 0.2 cycles, if the observation span is longer than 400 epochs. The ambiguities with big formal errors have usually short observation times and low elevation angles. Because the number of the available triple-frequency satellites is very limited at the moment, the observation time for each ambiguity on the double-difference level is in most of the cases relatively short. With more and more triple-frequency satellites and better calibrations of PCVs and DCBs between channels in the near future, we can expect a more reliable ambiguity resolution. Furthermore, if the Galileo E6 signal of more stations will become available, an improvement factor of two to three in total can be expected.

Acknowledgments This work was funded by ESA as part of the project (Satellite and Station Clock Modeling for GNSS, Reference: AO/1-6231/09/D/SR). We would like to thank M. Müller from the Institute of Geodesy and Photogrammetry, Eidgenössische Technische Hochschule Zürich (ETHZ) for processing the Galileo Two Line Element Set (TLE) (TLE 2012) and T.S. Kelso from CelesTrack for

providing TLE of the four Galileo satellites (GIOVE–A, GIOVE–B, GALILEO–PFM and GALILEO–FM2) for the time interval April 29, 2012 to May 9, 2012. We also want to thank IGS for providing triple-frequency M–GEX data on its archive (ftp://cddis.gsfc.nasa.gov/pub/gps/data/campaign/mgex/).

References

Cocard M, Bourgon S, Kamali O, Collins P (2008) A systematic investigation of optimal carrier-phase combinations for modernized triple-frequency GPS. J Geod 82(9):555–564. doi:10.1007/s00190-007-0201-x

Feng Y, Rizos C, Higgins M (2007) Multiple carrier ambiguity resolution and performance benefits for RTK and PPP positioning services in regional areas. In: Proceeding ION GNSS, Fort Worth, TX, USA, 25–28 Sept 2007, p 668–678

Gurtner W (2007) RINEX: The Receiver Independent Exchange Format Version 3.00. http://epic.awi.de/29985/1/Gur2007a.pdf

Hatch RR (2006) A new three-frequency, geometry-free, technique for ambiguity resolution. In: Proceeding ION GNSS, Ft Worth, TX, USA, 26–29 Sept 2006, p 309–316

Henkel P, Günther C (2010) Reliable integer ambiguity resolution with multi-frequency code carrier linear combinations. J Glob Pos Sys 9(2):90–103. doi:10.5081/jgps.9.2.90

Henkel P, Günther C (2012) Reliable integer ambiguity resolution: multi-frequency code carrier linear combinations and statistical a priori knowledge of attitude. J Inst Nav 59(1):61–75. doi:10.1002/navi.6

Januszewski J (2011) Satellite Navigation Systems, Data Messages, Data Transfer and Formats. In: Modern transport telematics: 11th International Conference on Transport System Telematics, TST 2011, Katowice-Ustroń, Poland, 19–22 Oct 2011, p 338–345 doi:10.1007/978-3-642-24660-9_39

Li B, Feng Y, Shen Y (2010) Three carrier ambiguity resolution: distance-independent performace demonstrated using semi-generated triple frequency GPS signals. GPS Solut 14(2):177–184. doi:10.1007/s10291-009-0131-6

Li J, Yang Y, Xu J, He H, Guo H (2012) Ionosphere-free combinations for triple-frequency GNSS with application in rapid ambiguity resolution over medium-long baselines. Proc China Sat Nav Conf (CSNC) 2012:173–187. doi:10.1007/978-3-642-29175-3_16

Inside GNSS (2012) First acquisition and tracking of IOV Galileo signals, vol 7, p 46–55. ISSN:1559–503X

Noll C, Bock Y, Habrich H, Moore A (2009) Development of data infrastructure to support scientific analysis for the international GNSS service. J Geod 83(3–4):309–325. doi:10.1007/s00190-008-0245-6

Weber R (2012) IGS M-GEX - The IGS Multi-GNSS Global Experiment. Wksp on GNSS Biases, 18–19 Jan 2012, Bern, Switzerland. http://www.biasws2012.unibe.ch/pdf/bws12_2.3.5.pdf

TLE (2012) Two line element set for Galileo satellites. http://www.celestrak.com/NORAD/elements/galileo.txt

USNO(2012) Block II satellite information. United States NAVAL Observatory (USNO). ftp://tycho.usno.navy.mil/pub/gps/gpsb2.txt

Wang Z, Liu J, Zhang K, (2004) Multiple carrier ambiguity resolution method for Galileo. In: Proceeding (2004) International Symposium GNSS/GPS. Australia, Sydney